Accepted Manuscript

Structural, stereochemical, and bioactive studies of cembranoids from Chinese soft coral *Sarcophyton trocheliophorum*

Lin-Fu Liang, Tibor Kurtán, Attila Mándi, Li-Gong Yao, Jia Li, Le-Fu Lan, Yue-Wei Guo

PII: S0040-4020(18)30219-9

DOI: 10.1016/j.tet.2018.02.059

Reference: TET 29330

To appear in: *Tetrahedron*

Received Date: 15 January 2018

Revised Date: 14 February 2018

Accepted Date: 23 February 2018

Please cite this article as: Liang L-F, Kurtán T, Mándi A, Yao L-G, Li J, Lan L-F, Guo Y-W, Structural, stereochemical, and bioactive studies of cembranoids from Chinese soft coral *Sarcophyton trocheliophorum*, *Tetrahedron* (2018), doi: 10.1016/j.tet.2018.02.059.

Graphical Abstract

To create your abstract, type over the instructions in the template box below.
Fonts or abstract dimensions should not be changed or altered.

Structural, Stereochemical, and Bioactive Studies of Cembranoids from Chinese Soft Coral *Sarcophyton trocheliophorum*

Leave this area blank for abstract info.

Lin-Fu Liang[a,b], Tibor Kurtán[d,*], Attila Mándi[d], Li-Gong Yao[b], Jia Li[b], Le-Fu Lan[b], Yue-Wei Guo[b,c,**]

[a] *College of Materials Science and Engineering, Central South University of Forestry and Technology, 498 South Shaoshan Road, Changsha 410004, P. R. China*

[b] *State Key Laboratory of Drug Research, Shanghai Institute of Materia Medica, Chinese Academy of Sciences, 555 Zu Chong Zhi Road, Zhang Jiang Hi-Tech Park, Shanghai 201203, P. R. China*

[c] *Open Studio for Drugability Research of Marine Natural Products, Qingdao National Laboratory for Marine Science and Technology, 1 Wenhai Road, Aoshanwei, Jimo, Qingdao 266237, P. R. China*

[d] *Department of Organic Chemistry, University of Debrecen, POB 400, 4002 Debrecen, Hungary*

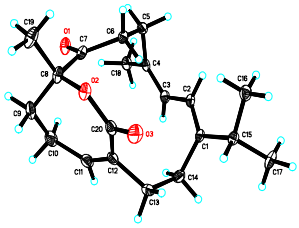

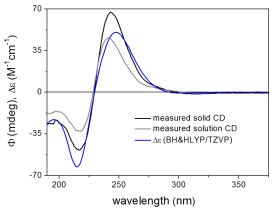

Tetrahedron
journal homepage: www.elsevier.com

Structural, Stereochemical, and Bioactive Studies of Cembranoids from Chinese Soft Coral *Sarcophyton trocheliophorum*

Lin-Fu Liang [a,b], Tibor Kurtán [d,*], Attila Mándi [d], Li-Gong Yao [b], Jia Li [b], Le-Fu Lan [b], Yue-Wei Guo [b,c,**]

[a]*College of Materials Science and Engineering, Central South University of Forestry and Technology, 498 South Shaoshan Road, Changsha 410004, P. R. China*
[b]*State Key Laboratory of Drug Research, Shanghai Institute of Materia Medica, Chinese Academy of Sciences, 555 Zu Chong Zhi Road, Zhang Jiang Hi-Tech Park, Shanghai 201203, P. R. China*
[c]*Open Studio for Drugability Research of Marine Natural Products, Qingdao National Laboratory for Marine Science and Technology, 1 Wenhai Road, Aoshanwei, Jimo, Qingdao 266237, P. R. China*
[d]*Department of Organic Chemistry, University of Debrecen, POB 400, 4002 Debrecen, Hungary*

ARTICLE INFO

Article history:
Received
Received in revised form
Accepted
Available online

Keywords:
Sarcophyton trocheliophorum
Cembranoid
Structure elucidation
Absolute configuration
Biological activities

ABSTRACT

A series of highly oxidative new cembranoids with diverse structural features such as a dienoate moiety (sarcophytonolides S – U, **1** – **3**) or an *α*,*β*-unsaturated *ε*-lactone (sartrolides H – J, **4** – **6**) were obtained from Hainan soft coral *Sarcophyton trocheliophorum*, along with known related analogues **7** – **13**. It is an extremely challenging work to determine the absolute configurations of these metabolites. For compounds **1**, **3** and **4**, solution TDDFT calculation of ECD and specific rotation were applied in combination with conformational analysis and NMR data to determine their relative and absolute configurations, leading to the revision of relative configuration of **14**. The absolute configurations of compounds **8** – **10** were determined by the solid-state TDDFT-ECD approach, and that of **8** was further confirmed by single-crystal X-ray diffraction experiment with Cu Kα radiation. In the bioassays, compound **8** exhibited not only moderate protein tyrosine phosphatase 1B (PTP1B) inhibitory activity (IC_{50} = 15.4 μM) but also moderate antibacterial activity against *Staphylococcus aureus* Newman strain (MIC_{50} = 250 μM).

1. Introduction

The soft corals of genus *Sarcophyton* (phylum Cnidaria, class Anthozoa, subclass Octocorallia, order Alcyonaceae, family Alcyoniidae) are abounded in the South China Sea, which have been reported to contain a variety of diterpenes, among which cembranes represent the most commonly encountered structural type. The cembranes possess a 14-membered carbocyclic skeleton containing one isopropyl and three methyl groups, in which methyl group was often oxidized to hydroxymethyl or carboxylic acid, further leading to the formation of lactone rings. This type of secondary metabolites not only display a library of diverse intriguing structural features, but also exhibit a wide spectrum of biological activities, including cytoprotective, cytotoxic, anti-inflammatory, and other bioactive properties,[1,2] making them attractive targets for chemical synthesis.[3,4]

The soft coral *Sarcophyton trocheliophorum* is a widespread member of the coral reef in the South China Sea. Recently, as part of our ongoing research project aimed at discovering bioactive substances from Chinese marine invertebrates,[5-9] we collected the title soft coral, off Yalong Bay, Hainan Province, China. Previous chemical studies on this organism by our group resulted in the identification of a novel class of cyclobutane-containing diterpenoids possessing PTP1B inhibitory activity,[5] two rare sarsolenane and three capnosane diterpenes with PTP1B inhibitory activity.[10] Inspired by the previous work, a subsequent detailed chemical investigation of another collection of the title animal was carried out, which led to the isolation of six new cembranolides, sarcophytonolides S – U (**1** – **3**) and sartrolides H – J (**4** – **6**), along with seven known related analogues **7** – **13**. In this paper we discuss the isolation and the structural elucidation of all the new compounds **1** – **6** and the stereochemical study for compounds **1**, **3**, **4** and **8** – **10**. For compounds **1**, **3** and **4**, solution TDDFT calculation of ECD was applied in combination with conformational analysis and NMR data to determine their relative and absolute configurations, leading to the revision of relative configuration of **14**. The absolute configurations of compounds **8** – **10** were determined by the solid-state TDDFT-ECD approach, and that of **8** was further confirmed by single-

* Corresponding authors. Tel./fax: +86-21-50805813; e-mail addresses: ywguo@simm.ac.cn (Y.-W. Guo). Tel: +36-52-512900; fax: +36-52-512744; e-mail addresses: kurtan.tibor@science.unideb.hu (T. Kurtán).

crystal X-ray diffraction experiment with Cu Kα radiation. This is first time to determine the absolute configurations of cembranoids with an *α*,*β*-unsaturated *ε*-lactone using TDDFT-ECD approach. In addition, the evaluations of their PTP1B inhibitory and antibacterial activities were reported herein.

2. Results and discussion

Freshly collected animals of *S. trocheliophorum* were immediately put at –20 °C, and kept frozen prior to extraction. The usual workup[5] of the Et_2O-soluble fraction of the acetone extract of the *S. trocheliophorum* yielded thirteen cembrane derivatives (**1** – **13**) (Fig. 1). Among them, seven known compounds were readily identified as deacetylemblide (**7**),[11] 4*Z*,12*Z*,14*E*-sarcophytolide (**8**),[12] sarcrassin D (**9**),[13] emblide (**10**),[11] sarcophytonolide A (**11**),[14] (*E*,*E*,*E*)-7,8-epoxy-l-isopropyl-4,8,12-trimethylcyclotetradeca-l,3,11-triene (**12**),[15] and (4*Z*,8*S*,9*R*,12*E*,14*E*)-9-hydroxy-1-isopropyl-8,12-dimethyloxabicyclo[9.3.2]-hexadeca-4,12,14-trien-18-one (**13**),[12] respectively, by comparison of their spectral data with those reported in the literature

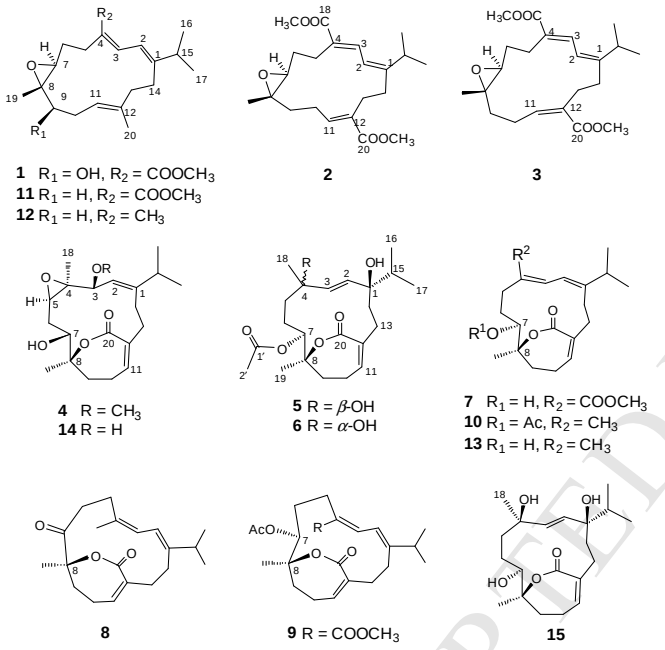

Fig. 1. The structures of compounds **1**−**15**.

A preliminary MS and ^{1}H NMR analysis revealed that six new compounds **1** – **6** should share a cembrane framework. The following careful analysis of ^{1}H and ^{13}C NMR data revealed that sarcophytonolides S – U (**1** – **3**) possessed a dienoate moiety (C-1 – C-4 and C-18), whereas sartrolides H – J (**4** – **6**) had a lactone ring, namely an *α*,*β*-unsaturated *ε*-lactone (C-8 – C-12 and C-20). The planar structures and relative configuration of compounds **1** – **6** have been elucidated by means of a detailed 1D and 2D NMR analysis aided by comparison with data of related derivatives, and their absolute configurations were determined by TDDFT-ECD approach. Herein we will describe firstly the structural analyses of epoxidic cembranes **1** – **3** followed by those of the lactonic cembranes **4** – **6**.

Sarcophytonolide S (**1**) was isolated as colorless oil. Its molecular formula $C_{21}H_{32}O_4$ was deduced from its HR-ESI-MS ($[M + Na]^+$ at *m*/*z* 371.2172). Thus, six degrees of unsaturation were determined for **1**. Compound **1** exhibited IR absorptions indicative of the presence of hydroxyl and ester carbonyl moieties (ν_{max} 3498, 1713 cm^{-1}).[14] An intense UV absorption at λ_{max} 283 nm (log ε 3.33) indicated the presence of a dienoate moiety,[14] which was confirmed by ^{1}H and ^{13}C NMR data of **1**: δ_C 158.1 (*s*, C-1), 119.5 (*d*, C-2), 136.6 (*d*, C-3), 126.2 (*s*, C-4), 168.0 (*s*, C-18), 51.4 (*q*, C-1′) and δ_H 6.88 (*d*, *J* = 11.5 Hz, H-2), 6.67 (*d*, *J* = 11.5 Hz, H-3), 3.77 (*s*, Me-1′). Its NMR spectra also indicated the presence of an isolated trisubstituted double bond [δ_C 118.8 (*d*, C-11), 137.6 (*s*, C-12) and δ_H 5.03 (*td*, *J* = 7.2, 1.2 Hz, H-11)], a trisubstituted epoxidic ring [δ_C 62.7 (*d*, C-7), 63.5 (*s*, C-8), δ_H 2.86 (*dd*, *J* = 6.6, 5.2 Hz, H-7)] and an oxymethine [δ_C 78.0 (*d*, C-9) and δ_H 3.16 (*dd*, *J* = 8.8, 6.1 Hz, H-9)] (see *Experimental Section*). Comparison of these data with those of co-isolated cembranoid sarcophytonolide A (**11**), previously reported by our group,[14] suggested that **1** and **11** actually share the same carbon framework and they only differ in the presence of a hydroxyl group at C-9 of **1**, in agreement with the 16 mass units difference. This was confirmed further by the HMBC correlations of Me-19/C-7, C-8, and C-9, and H-7/C-9 (Fig. 2). The geometry of the Δ^1, Δ^3, and Δ^{11} double bonds, were suggested to be the same as in **12** on the basis of the almost identical chemical shift values for C-1 – C-4, C-11, C-12, and C-20 in these two compounds. The relative configuration of the three stereogenic centers C-7, C-8 and C-9 was tentatively established as (7*R**,8*R**,9*S**) by the ROESY correlations of H-7/H-9, H-7/H_a-6 and Me-19/H_b-6 in its ROESY spectrum (Fig. 2). Unfortunately, the attempt to determine the absolute configuration of **1** through the Mosher's method failed indeed, due to the insufficient amount to apply the method.

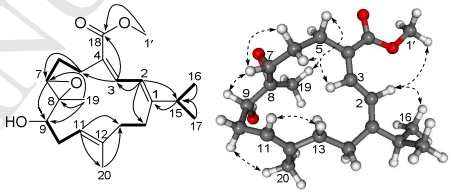

Fig. 2. The ^{1}H,^{1}H-COSY, HMBC, and ROESY correlations of compound **1**.

Instead, the solution TDDFT-ECD calculation method was applied, the efficiency of which has been demonstrated earlier in the stereochemical studies of conformationally flexible macrolides.[16,17] Since elucidation of the relative configuration of **1** was tentative, we investigated *in silico* two diastereomers, the (7*S*,8*S*,9*R*)-**1** and the (7*S*,8*S*,9*S*)-**1** in order to confirm the assignment of the relative configuration. The initial MMFF (Merck Molecular Force Field) conformational analysis of (7*S*,8*S*,9*R*)-**1** resulted in 300 conformers (Fig. S41), while that of (7*S*,8*S*,9*S*)-**1** gave 339 conformers (Fig. S42). These geometries were reoptimized by various DFT methods [B3LYP/6-31G(d) *in vacuo*, B3LYP/TZVP with PCM for MeCN, B97D/TZVP[16,18] with PCM for MeCN and CAM-B3LYP/TZVP[19,20] with PCM for MeCN] and ECD spectra were computed at the B3LYP/TZVP, BH&HLYP/TZVP, CAM-B3LYP/TZVP and PBE0/TZVP levels. Interestingly, for both diastereomers we got opposite results by using different sets of DFT conformers. While gas-phase calculations for both diastereomers suggested (*S*) absolute configuration for the chirality centers C-7 and C-8, the B97D functional suggested opposite absolute configuration. In the case of (7*S*,8*S*,9*R*)-**1**, the solvent model B3LYP and CAM-B3LYP reoptimizations yielded similar ECD spectra to the gas-phase calculations (Fig. 3), while for (7*S*,8*S*,9*S*)-**1** the experimental high-wavelength intense positive Cotton effect (CE) was computed negative but the low-wavelength one was found positive at these levels (Fig. 4).

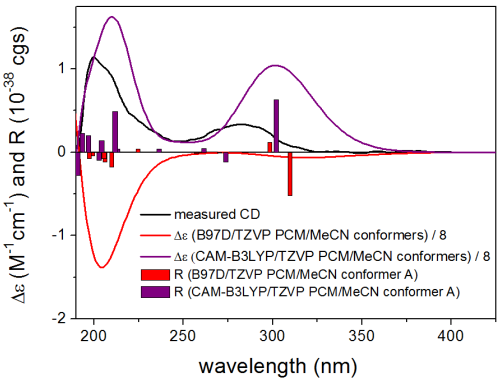

Fig. 3. Experimental ECD spectrum of **1** in MeCN compared with the Boltzmann-weighted B3LYP/TZVP PCM/MeCN spectra of the B97D/TZVP PCM/MeCN conformers (red line, 8 conformers over 1%) and the CAM-B3LYP/TZVP PCM/MeCN conformers (purple line, 21 conformers over 1%) of (7*S*,8*S*,9*R*)-**1**. Bars represent the rotational strength values of the lowest-energy conformers.

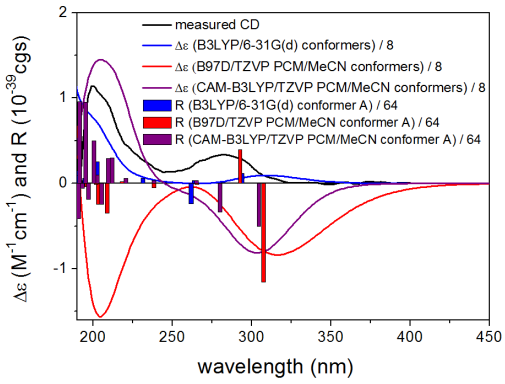

Fig. 4. Experimental ECD spectrum of **1** in MeCN compared with the Boltzmann-weighted B3LYP/TZVP spectrum of the B3LYP/6-31G(d) conformers (blue line, 19 conformers over 1%), B3LYP/TZVP PCM/MeCN spectra of the B97D/TZVP PCM/MeCN conformers (red line, 13 conformers over 1%) and the CAM-B3LYP/TZVP PCM/MeCN conformers (purple line, 26 conformers over 1%) of (7*S*,8*S*,9*S*)-**1**. Bars represent the rotational strength values of the lowest-energy conformers.

These contradicting results derived from the rather different Boltzmann-distribution of the conformers estimated by the different methods and ECD spectra were found highly sensitive to the conformation of the macrocycle.[16] For the configurational assignment of highly flexible derivatives, it is advisable and helpful to apply the combination of more than one chiroptical method.[21,22] Thus conformers were also reoptimized with PCM for $CHCl_3$ and optical rotation (OR) values were computed for the gas-phase and the PCM/$CHCl_3$ optimized conformers.[23] For most low-energy conformers, ECD and OR calculations suggested the same absolute configuration or the overall OR value was too small to be decisive. On the basis of the computed ECD spectra of the two diastereomers at the same levels, it could be nevertheless concluded that ECD (and also OR) is mainly influenced by the epoxide moiety and the 9-OH has minor contribution. Since the combination of ECD and OR calculations was not sufficient to distinguish the two diastereomers, we investigated the low-level DFT optimized conformers obtained at various levels and checked the feasibility of the experimental ROESY effects. Most of the low-energy conformers of (7*S*,8*S*,9*S*)-**1** would not give ROE effect between H-7 and H-9 because of the large interatomic distance (see global minima on Fig. S42 as reference), and this is also true for most of the B97D optimized geometries of the other diastereomer (Fig. S41a). The ROESY correlations were in agreement with the conformational distribution of the B3LYP gas-phase, solvent model and CAM-B3LYP reoptimization of (7*S*,8*S*,9*R*)-**1** (Fig. S41b) and thus the (7*S*,8*S*,9*R*) absolute configuration was suggested for **1**. This assignment is also in line with the results obtained for the biosynthetically related compound **3** (*vide infra*).

Table 1. ^{1}H (400 MHz) and ^{13}C NMR (100 MHz) data for compounds **1 – 3** (in $CDCl_3$).

No	**1**		**2**		**3**	
	δ_H	δ_C	δ_H	δ_C	δ_H	δ_C
1		158.1 (*s*)		158.8 (*s*)		158.6 (*s*)
2	6.89 (*d*, 11.4)	119.5 (*d*)	6.23 (*d*, 12.1)	120.3 (*d*)	6.22 (*d*, 12.0)	118.8 (*d*)
3	6.67 (*dt*, 11.4, 1.1)	136.6 (*d*)	7.70 (*d*, 12.1)	134.3 (*d*)	7.60 (*d*, 11.9)	136.5 (*d*)
4		126.2 (*s*)		127.8 (*s*)		127.6 (*s*)
5a	2.55 (7.3, 2.9)	30.7 (*t*)	2.60 (*m*)	23.2 (*t*)	2.63 (*m*)	23.6 (*t*)
5b			2.56 (*m*,)		2.60 (*m*)	
6a	1.95 (*m*)	26.6 (*t*)	2.06 (*m*)	27.1 (*t*)	1.90 (*m*)	26.8 (*t*)
6b	1.76 (*m*)		1.58 (*m*)		1.68 (*m*)	
7	2.86 (*dd*, 6.6, 5.1)	62.7 (*d*)	2.86 (*dd*, 9.7, 3.5)	60.6 (*d*)	2.65 (*t*, 5.6)	62.7 (*d*)
8		63.5 (*s*)		60.9 (*s*)		61.0 (*s*)
9a	3.16 (*dd*, 8.7, 6.0)	78.0 (*d*)	1.81 (*m*)	36.1 (*t*)	1.65 (*m*)	36.2 (*t*)
9b			1.48 (*m*)		1.18 (*m*)	
10a	2.33 (*m*)	31.6 (*t*)	2.15 (*m*)	24.2 (*t*)	2.16 (*m*)	23.9 (*t*)
10b			2.02 (*m*)		2.02 (*m*)	
11	5.03 (*td*, 7.1, 1.2)	118.8 (*d*)	6.80 (*t*, 7.6)	142.5 (*d*)	6.59 (*dd*, 7.6, 4.2)	144.4 (*d*)
12		137.6 (*s*)		132.3 (*s*)		130.0 (*s*)
13a	2.27 (*m*)	39.1 (*t*)	2.61 (*m*)	27.6 (*t*)	2.81 (*m*)	26.9 (*t*)
13b	2.10 (*m*)		2.43 (*m*)		2.42 (*m*)	
14a	2.38 (*m*)	27.3 (*t*)	2.40 (*m*)	29.8 (*t*)	2.67 (*m*)	28.8 (*t*)
14b	2.33 (*m*)		2.27 (*m*)		2.34 (*m*)	
15	2.39 (*m*)	35.3 (*d*)	3.19 (*m*)	29.7 (*d*)	2.00 (*m*)	36.7 (*d*)
16	1.07 (*d*, 6.8)	22.0 (*q*)	0.94 (*d*, 6.8)	20.3 (*q*)	0.98 (*d*, 6.8)	22.2 (*q*)
17	1.07 (*d*, 6.8)	21.7 (*q*)	1.00 (*d*, 6.8)	21.2 (*q*)	1.07 (*d*, 6.8)	20.7 (*q*)
18		168.0 (*s*)		168.7 (*s*)		168.5 (*s*)
19	1.27 (*s*)	10.7 (*q*)	1.17 (*s*)	17.9 (*q*)	1.10 (*s*)	16.8 (*q*)
20	1.66 (*d*, 0.9)	16.9 (*q*)		168.0 (*s*)		167.7 (*s*)
1´	3.77 (*s*)	51.4 (*q*)	3.76 (*s*)	51.8 (*q*)	3.74 (*s*)	51.8 (*q*)

2´	3.74 (s)	51.8 (*q*)	3.76 (s)	51.7 (*q*)

Sarcophytonolide T (**2**), a colorless oil, had the same molecular formula $C_{22}H_{32}O_5$ as that of sarcophytonolides B[14] and O[24], established by HR-ESI-MS ([M + Na]$^+$ at *m/z* 399.2172). Analysis of the NMR data for **2** (Table 1) revealed the presence of the same functionalities as that of sarcophytonolide B, such as a dienoate moiety [δ_C 168.5 (*s*, C-18), 51.8 (*q*, C-1´), 158.8 (*s*, C-1), 120.3 (*d*, C-2), 134.3 (*d*, C-3), 127.8 (*s*, C-4), and δ_H 3.76 (*s*, Me-1´), 6.23 (*d*, *J* = 12.1 Hz, H-2), 7.70 (*d*, *J* = 12.1 Hz, H-3)], an *α*,*β*-conjugated methyl ester [δ_C 167.7 (*s*, C-20), 51.8 (*q*, C-2´), 142.5 (*d*, C-11), 132.3 (s, C-12), and δ_H 3.74 (*s*, Me-2´), 6.80 (*t*, *J* = 7.6 Hz, H-11)], an epoxide moiety [δ_C 60.6 (*d*, C-7), 60.9 (*s*, C-8), and δ_H 2.86 (*dd*, *J* = 9.7, 3.5 Hz, H-7)]. The detailed inspection of 2D NMR spectra (Fig. 5) revealed that **2** also shared the same carbon skeleton with sarcophytonolide B.[14] The NOE interactions of H-2/H_b-14 and H-3/H-15 together with the s-*trans* orientation of H-2 and H-3 ($J_{H\text{-}2,H\text{-}3}$ = 12.1 Hz) indicated a (*Z*) configuration for Δ^1 and an *E*-configuration for Δ^3. The *E*-configuration for Δ^{11} was deduced from the ROESY correlation of H_a-10/H_a-13 (Fig. 5). Thus, the geometry of the three double bonds within the cembrane ring of **2** is the opposite to that of sarcophytonolides B and O. Experimental ECD spectrum of **2** showed only weak CEs, which were not suitable for an unambiguous TDDFT-ECD study and due to the conformational flexibility, the +42 specific rotation value could not be safely used to elucidate absolute configuration either. It can only suggest the same absolute configuration for C-7 and C-8 chirality centers than in **1** and **3**. Based on biosynthetic considerations, the related **1** – **3** are homochiral for the corresponding chirality centers, and thus (7*S*,8*S*)-**2** absolute configuration could be tentatively assigned.

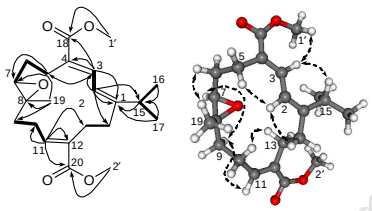

Fig. 5. ^{1}H,^{1}H-COSY, HMBC, and ROESY correlations of compound **2**.

Sarcophytonolide U (**3**) was isolated as colorless oil. Its molecular formula $C_{22}H_{32}O_5$ was deduced from the quasi-molecular ion at *m/z* 399.2176 in the HR-ESI-MS. Thus, seven degrees of unsaturation were determined for **3**. Its IR [ν_{max} 1716, 1636 cm^{-1}], NMR signals [δ_C 168.5 (*s*, C-18), 167.7 (*s*, C-19), 51.8 (*q*, C-1´), 51.7 (*q*, C-2´) and δ_H 3.74 (*s*, Me-1´), 3.76 (*s*, Me-2´)], and UV [λ_{max} (log ε) 286 (3.97), 238 (3.82) nm] suggested the presence of two *α*,*β*-unsaturated methyl ester moieties. NMR signals also revealed the presence of three trisubstituted double bonds [δ_C 158.6 (*s*, C-1), 118.8 (*d*, C-2), 136.5 (*d*, C-3), 127.6 (*s*, C-4), 144.4 (*d*, C-11), 130.0 (*s*, C-12) and δ_H 6.22 (*d*, *J* = 12.0 Hz, H-2), 7.60 (*d*, *J* = 11.9 Hz, H-3), 6.59 (*t*, *dd* = 7.6, 4.2 Hz, H-11)]; an epoxymethine [δ_C 62.7 (*d*, C-7) and δ_H 2.65 (*t*, *J* = 5.6 Hz, H-7)]; an epoxyde quaternary carbon [δ_C 61.0 (*s*, C-8)]; an isopropyl group [δ_H 0.98 (*d*, *J* = 6.8 Hz, Me-16), 1.07 (*d*, *J* = 6.8 Hz, Me-17), 2.00 (1H, *m*, H-15)]; and a methyl group [δ_H 1.10 (*s*, Me-19)] (Table 1). The NMR data of **3** were almost identical with those of sarcrassin A,[13] one cembrane diterpenoid previously isolated from the Hainan soft coral *Sarcophyton crassocaule*. However, the sign of the $[\alpha]_D^{22}$ value of **3** [+355.5 (*c* = 0.11, $CHCl_3$)] had opposite sign to that of sarcrassin A {$[\alpha]_D^{20}$ – 6.3 (*c* = 0.208, $CHCl_3$)} with significantly different magnitude. It is essential to point out that there is a misprint or mistake for the ^{13}C NMR data of C-8 in sarcrassin A (δ_C 66.8).[13] The chemical shift of the epoxidic quaternary carbon C-8 of cembranes from the genus *Sarcophyton* was usually observed in the range of δ_C 59.0 – 64.0 ppm, and the remarkably difference between the chemical shifts of C-7 and C-8 in sarcrassin A (Δ 4.7 ppm) is not justified.[1,2] Compared with structurally closely related sarcrassin B reported in the same paper,[13] ^{13}C chemical shift of C-8 of sarcrassin A may have to be shifted to δ_C 60.8 or 61.8 reasonably, which is similar to that of **3**.

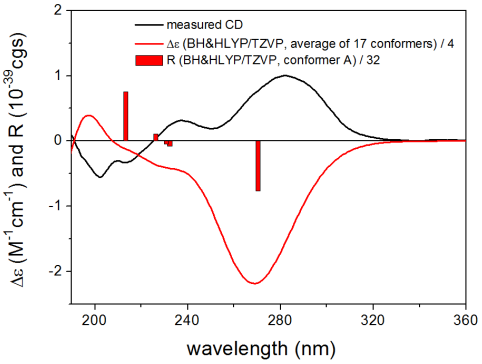

Fig. 6. Experimental ECD spectrum of **3** in MeCN compared with the BH&HLYP/TZVP ECD spectrum computed for the B3LYP/6-31G(d) *in vacuo* conformers of (7*R*,8*R*)-**3**. Bars represent computed rotational strengths of the lowest-energy conformer.

In order to determine the absolute configuration of **3**, the same calculation protocol was pursued as for **1**. The conformational analysis was carried out with DFT reoptimizations at B3LYP/6-31G(d) *in vacuo* (Fig. S43), B3LYP/TZVP PCM/MeCN and B97D/TZVP PCM/MeCN levels and ECD calculations with B3LYP, BH&HLYP and PBE0 functionals on the arbitrarily chosen (7*R*,8*R*)-**3**. Despite the markedly lower conformational flexibility (88 MMFF conformers) of **3**, ECD spectra computed with various functionals for the different sets of DFT optimized geometries were rather versatile. The characteristic 280 nm positive experimental ECD transition was reproduced with a negative sign in all the combinations suggesting (7*S*,8*S*) absolute configuration but acceptable overall mirror image agreement was found only by the BH&HLYP/TZVP level ECD calculations performed on the B3LYP/6-31G(d) *in vacuo* conformers (Fig. 6). Many other combinations showed partial agreement and partial mirror-image agreement simultaneously indicating a possible Boltzmann-population error, which seemed decisive for the computed ECD curves. OR values were also computed at the same levels as for **1**. All the 3 applied levels for all 3 sets of DFT reoptimizations resulted in large negative average values and all solvent model calculations yielded only conformers with negative OR value over 1.5% population, verifying the ECD results and allowing the unambiguous elucidation of the absolute configuration as (7*S*,8*S*).

The HR-ESI-MS data for sartrolide H (**4**) indicated the molecular formula $C_{21}H_{32}O_5$, differing from that of sartrolide C (**14**)[25] in a CH_2 residue. Analysis of its spectral data clearly indicated that two molecules shared the presence of an (*E*)-C=C bond [δ_C 152.5 (*s*, C-1), 119.6 (*d*, C-2), and δ_H 5.38 (1H, *d*, *J* = 9.5 Hz, H-2)], an epoxide moiety [δ_C 63.1 (*s*, C-4), 60.2 (*d*, C-5), and δ_H 2.98 (1H, *dd*, *J* = 10.4, 4.3 Hz, H-5], a hydroxymethine [δ_C 69.1 (*d*, C-7) and δ_H 4.08 (1H, *d*, *J* = 11.6 Hz, H-7)], and an *α*,*β*-unsaturated *ε*-lactone [δ_C 166.3 (*s*, C-20), 141.2 (*d*, C-11), 132.4 (*s*, C-12), 82.9 (*s*, C-8), and δ_H 6.21 (*t*, *J* = 4.6 Hz, H-11)] (see *Experimental Section*). Careful comparison of NMR spectra of **4** and **14** located the differences at C-3, where an –OMe group in **4** linked instead of an –OH group in **14**, which was further

supported by the characteristic HMBC correlation of Me-1´/C-3 (Fig. 7). In agreement with methylation at OH–C-3, the chemical shift of C-3 was downfield shifted (from δ_C 66.7 to 75.4).[26] The pattern of coupling constants and ROESY correlations detected for **4** exactly paralleled with those of **14**, thus indicating that the two molecules shared the same relative configuration. Since the use of methanol was avoided during the entire extraction/purification procedure of the organism, an artifact nature of the methyl ether group present in **4** can be excluded.

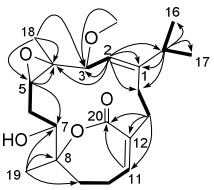

4

Fig. 7. The ^{1}H,^{1}H-COSY and HMBC correlations of compound **4**.

Reoptimization of the 81 MMFF conformers of (3*S*,4*R*,5*R*,7*R*,8*R*)-**4** at B3LYP/6-31G(d) *in vacuo*, B97D/TZVP PCM/MeCN and CAM-B3LYP/TZVP PCM/MeCN levels resulted in 3, 15 and 25 conformers over 1%, respectively (Fig. S44). Both the gas-phase and solvent model ECD calculations (Fig. S45) gave very bad and contradictory agreement with the experimental ECD and low-energy conformers were not in line with the NOE correlations found in the earlier work[25] for **14** (especially H-3/H-14a, H-3/H-6b and H-7/Me-19 seemed to be difficult to be present simultaneously). It seems that due to the flexibility of the macrocycle, NOE correlations of H-3 are not decisive for the relative configuration and thus (3*R**,4*R**,5*R**,7*R**,8*R**) relative configuration may be also possible. Indeed, the 79 MMFF conformers reoptimized at the above three levels gave low-energy conformers (Fig. S46) in accordance with the characteristic NOE correlations reported for **14** and ECD calculations computed for each sets of conformers at various levels gave univocally moderate to good agreement with the experimental ECD spectrum (Fig. 8) allowing to modify the relative configuration of **14** and elucidate the absolute configuration of **4** as (3*R*,4*R*,5*R*,7*R*,8*R*). It is interesting to note that B97D functional performed the best for DFT optimization while it had problems for **1** and **3** underlining that there is no superior level of theory for computing chiroptical parameters and more than one level is recommended to test for flexible systems.[16,27]

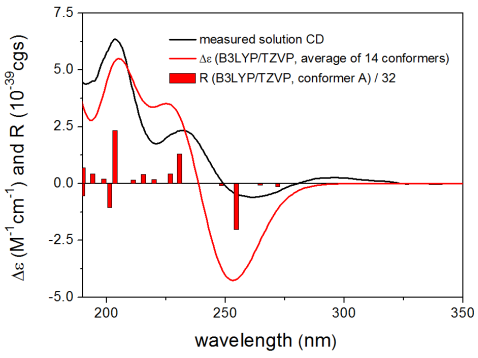

Fig. 8. Experimental ECD spectrum of **4** in MeCN (black) compared with the Boltzmann-weighted B3LYP/TZVP PCM/MeCN ECD spectrum of (3*R*,4*R*,5*R*,7*R*,8*R*)-**4** (red) computed for the B97D/TZVP PCM/MeCN conformers. Bars represent computed rotational strengths of the lowest-energy conformer.

Table 2. ^{1}H (400 MHz) and ^{13}C NMR (100 MHz) data for compounds **5** and **6** (in $CDCl_3$).

No	**5**		**6**	
	δ_H	δ_C	δ_H	δ_C
1		75.9 (*s*)		74.7 (*s*)
2	5.48 (*d*, 16.6)	134.6 (*d*)	5.71 (*d*, 15.7)	134.5 (*d*)
3	5.53 (*d*, 16.6)	132.9 (*d*)	5.59 (*d*, 15.7)	133.9 (*d*)
4		73.4 (*s*)		74.0 (*s*)
5a	1.73 (*m*)	35.2 (*t*)	1.70 (*m*, H_a)	35.3 (*t*)
5b	1.67 (*m*)		1.64 (*m*, H_b)	
6a	1.84 (*m*)	25.1 (*t*)	1.80 (*m*, H_a)	24.0 (*t*)
6b	1.66 (*m*)		1.69 (*m*, H_b)	
7	5.29 (*d*, 9.9)	71.6 (*d*)	5.47 (*d*, 10.6, 1.8)	73.5 (*d*)
8		82.9 (*s*)		82.7 (*s*)
9a	2.02 (*m*)	36.1(*t*)	2.08 (*m*, H_a)	34.1 (*t*)
9b	1.98 (*m*)		1.98 (*m*, H_b)	
10a	2.79 (*m*)	24.2 (*t*)	2.85 (*m*, H_a)	27.2 (*t*)
10b	1.96 (*m*)		1.43 (*m*, H_b)	
11	6.48 (*t*, 4.5)	141.9 (*d*)	6.34 (*t*, 4.5)	143.6 (*d*)
12		133.8 (*s*)		134.0 (*s*)
13a	3.05 (*t*, 13.0)	30.6 (*t*)	2.93 (*t*, 13.7, H_a)	31.8 (*t*)
13b	2.19 (*m*)		2.20 (*m*, H_b)	
14a	1.88 (*m*)	39.0 (*t*)	1.98 (*m*, H_a)	37.8 (*t*)
14b	1.84 (*m*)		1.81 (*m*, H_b)	
15	1.69 (*m*)	37.5 (*d*)	1.77 (*m*)	39.8 (*d*)
16	0.86 (*d*, 6.8)	17.3 (*q*)	0.85 (*d*, 6.8)	16.9 (*q*)
17	0.80 (*d*, 6.8)	16.3 (*q*)	0.88 (*d*, 6.8)	16.8 (*q*)
18	1.24 (*s*)	32.3 (*q*)	1.23 (*s*)	32.2 (*q*)
19	1.39 (*s*)	23.7 (*q*)	1.37 (*s*)	23.4 (*q*)
20		168.5 (*s*)		168.5 (*s*)
1´		171.4 (*s*)		171.1 (*s*)
2´	2.10 (*s*)	21.3 (*q*)	2.12 (*s*)	21.3 (*q*)

Sartrolide I (**5**), a colorless oil, had the same molecular formula $C_{22}H_{32}O_5$ as that of sartrolide D (**15**),[25] according to the HR-ESI-MS ($[M + Na]^+$ at *m/z* 415.2076), which was corresponding to an additional C_2H_2O unit compared to **15** and indicating one degree of unsaturation more than **15**. Inspection of ^{1}H and ^{13}C NMR spectral data of **5** (Table 2), aided by 2D NMR experiments (Fig. 9), indicated the presence of an *α*,*β*-unsaturated *ε*-lactone moiety (C-8–C-12 and C-20), an (*E*)-C=C bond (C-2 and C-3), and two oxygenated quaternary carbons (C-1 and C-4), which were the same as in **15**. Careful comparison of the NMR data of **5** and **15** revealed that the only difference between them resided in the replacement of the –OH group at C-7 with an –OAc group, as clearly indicated by the significant downfield shift of H-7 (from δ_H 4.44 in **15** to 5.29 in **5**) and by its HMBC cross-

peak of H-7/C-1´ (Fig. 9). Its ROESY cross-peaks of H-3/Me-16 and Me-18 revealed that the isopropyl group and Me-18 were co-facial (*α*) (Fig. 9). The pattern of coupling constants and NOESY correlations detected for the residue partial structure of **5** (Fig. 9) were similar to those of **15**, thus indicating that the two molecules shared the same relative configurations for the corresponding chiral centers. Hence, the isolate **5** was the corresponding 7-*O*-acetyl derivative of **15**. Unfortunately, acetylation of **15** using acetic anhydride/pyridine or dichloromethane was failed, probably due to the steric hindrance around the secondary OH group.

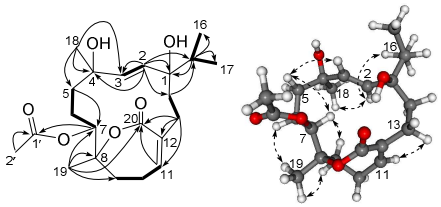

Fig. 9. The ^{1}H,^{1}H-COSY, HMBC, and ROESY correlations of compound **5**.

Sartrolide J (**6**) possessed the same molecular formula $C_{22}H_{34}O_6$ as that of sartrolide I (**5**), as deduced from the quasi-molecular ion at *m/z* 417.2269 in the HR-ESI-MS. Inspection of NMR data of **6** (Table 2) revealed that the planar structure of **6** should be the same as that of **5**. The ROESY correlations of H-2/Me-17 and H-3/Me-18 revealed different orientations of the isopropyl group and Me-18 in **6**, which were different from those of **5**. Referred to the above mentioned general rule,[28,29] the configuration at C-1 of **6** was tentatively assigned as *α*, and subsequently *β*-orientation for Me-18. Hence, the isolate **6** was the corresponding 7-*O*-acetyl derivative of 4-*epi*-**15**.

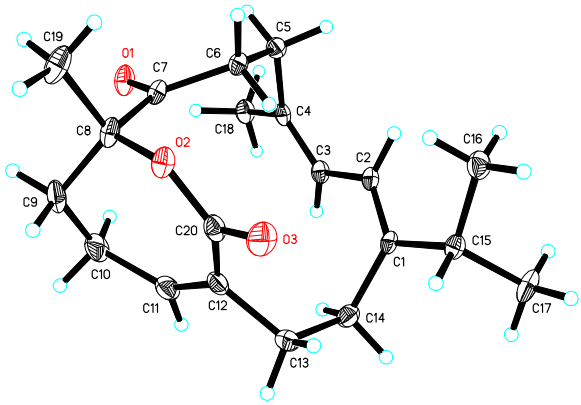

Fig. 10. Perspective drawing of the X-ray structure of compound **8**.

Due to the flexibility of the cembrane, it is an extremely challenging work to determine the absolute configurations of these metabolites. Since our attempts to upgrade the relative configurations around the 14-membered cembrane rings of sarcophytonolides S – U (**1** – **3**) and sartrolides H – J (**4** – **6**) to the absolute ones through the Mosher's method had failed, we tried to get crystals for application of X-ray crystallography along with the solution TDDFT approach. Given the higher amounts available, these attempts proved to be successful for the three known compounds, 4*Z*,12*Z*,14*E*-sarcophytolide (**8**), sarcrassin D (**9**), emblide (**10**), which were re-crystallized from methanol. Among them, the absolute configurations of **9** and emblide **10** was regained in this research, which had been elucidated by single-crystal X-ray diffraction experiment with Cu Kα (*λ* = 1.54178 Å) radiation previously by our group.[25] Similarly, the absolute configuration of **8** was assigned to be 8*R*, suggested by the Flack parameter [–0.03(17)] (Fig. 10). Noteworthy, the three compounds **8** – **10** share the *R* configuration at C-8, the joining point of the *α*,*β*-unsaturated *ε*-lactone moiety within the cembrane ring.

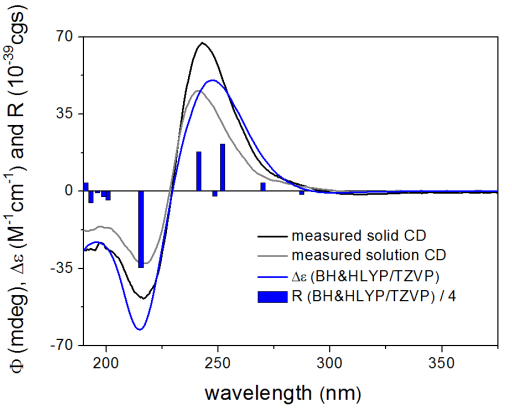

Fig. 11. Solution (acetonitrile, grey curve) and solid-state (black curve) ECD spectra of (+)-(8*R*)-4*Z*,12*Z*,14*E*-sarcophytolide (**8**) compared with the computed BH&HLYP/TZVP (blue) spectrum calculated for X-ray geometry of (8*R*)-**8**. Bars represent computed rotational strengths.

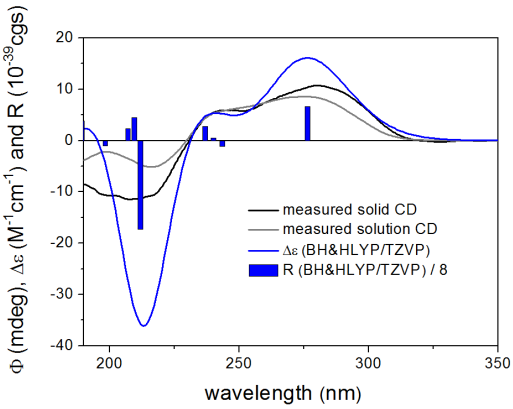

Fig. 12. Solution (acetonitrile, grey curve) and solid-state (black curve) ECD spectra of (+)-(7*S*,8*R*)-sarcrassin D (**9**) compared with the computed BH&HLYP/TZVP (blue) spectrum calculated for X-ray geometry of (7*S*,8*R*)-**9**. Bars represent computed rotational strengths.

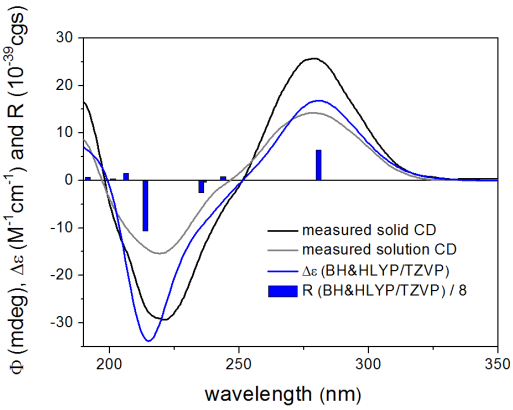

Fig. 13. Solution (acetonitrile, grey curve) and solid-state (black curve) ECD spectra of (+)-(7*S*,8*R*)-emblide (**10**) compared with the computed BH&HLYP/TZVP (blue) spectrum calculated for X-ray geometry of (7*S*,8*R*)-**10**. Bars represent computed rotational strengths.

Furthermore, the absolute configurations of compounds **8** – **10** were confirmed by the solid-state TDDFT-ECD approach. The solid-state TDDFT-ECD method is a powerful tool, and has been tested and utilized for the configurational assignment of numerous natural products.[30-32] The ECD spectra of (+)-**8**, (+)-**9**, and (+)-**10** were recorded in both acetonitrile solution and as KCl disk, which showed similar profiles (Fig. 11 – 13), suggesting that similar conformers are prevalent in solution and the solid-state (For descriptions referring characteristic bands in their ECD spectra see Text S1). The X-ray geometries of compounds **8** – **10** were optimized at the B3LYP/6-31G(d) DFT level *in vacuo* (Fig. S47 – 49) for the solid-state TDDFT-ECD method,. These structures were employed for TDDFT calculations with various functionals (B3LYP, BH&HLYP and PBE0) and TZVP basis set to check the consistency of the calculations. The CD spectrum calculated with the TDDFT method at the BH&HLYP/TZVP level, using as input geometry the X-ray coordinates for **8** – **10** with (8*R*), (7*S*,8*R*) and (7*S*,8*R*) configurations, respectively, is shown in Fig. 11 – 13. It clearly reproduced well the shapes of the main experimental bands, except for some intensity overestimation. Thus the absolute configurations of (+)-4*Z*,12*Z*,14*E*-sarcophytolide (**8**), (+)-sarcrassin D (**9**), and (+)-emblide (**10**) were determined as (+)-(8*R*)-**8**, (+)-(7*S*,8*R*)-**9**, and (+)-(7*S*,8*R*)-**10**.

Compounds **1** – **8** were tested for their inhibitory activity against protein tyrosine phosphatase 1B (PTP1B), a key target for the treatment of Type-II diabetes and obesity.[33] The result showed that compounds **4** and **8** exhibited moderate PTP1B inhibitory activity (IC_{50}'s = 19.9 ± 3.13 and 15.4 ± 1.11 μM, respectively), of which compound **8** exhibited the strongest inhibitory activity, but less than that of positive control oleanolic acid (IC_{50} = 2.6 μM). In addition, compound **8** also exhibited moderate antibacterial activity against *Staphylococcus aureus* Newman strain (MIC_{50} = 250 μM).

Due to the scarcity of the new products, biomimetic total synthesis and chemical correlation should be conducted in future to understand their biosynthetic origins and their biological role in the life cycle of the soft coral, which would be helpful for further specific pharmacological studies.

In conclusion, thirteen cembrane derivatives (**1** – **13**) with diverse structural features were isolated from animals of *S. trocheliophorum*. Structurally, these cembranoids can be classified into two subclasses: one subclass consisited of sarcophytonolides S – U (**1** – **3**) which possessed a dienoate moiety including (C-1 – C-4 and C-18), whereas the other subclass comprised by sartrolides H – J (**4** – **6**) which had an *α,β*-unsaturated *ε*-lactone (C-8 – C-12 and C-20). Our results provide further evidences about the chemical diversity of this distinct group of diterpenes produced by the title animals. For compounds **1**, **3** and **4**, solution TDDFT calculation of ECD and specific rotation was applied in combination with conformational analysis and NMR data to determine the relative and absolute configuration, leading to the revision of relative configuration of **14**. The absolute configurations of compounds **8** – **10** were determined by the solid-state TDDFT-ECD approach, and that of **8** was further confirmed by single-crystal X-ray diffraction experiment with Cu Kα radiation. This is first time to determine the absolute configurations of above cembranoids using TDDFT-ECD approach. Among the isolates, compounds **4** and **8** exhibited moderate PTP1B inhibitory activity, and compound **8** also exhibited moderate antibacterial activity.

3. Experimental section

3.1. General experimental procedures

Optical rotations were measured on a Perkin-Elmer 241MC polarimeter. UV spectra were recorded on a Varian Cary 300 Bio spectrophotometer. IR spectra were recorded on a Nicolet-Magna FT-IR 750 spectrometer. NMR spectra were measured on either a Bruker DRX-500 or a Bruker DRX-400 spectrometer with the residual $CHCl_3$ (δ_H 7.26 ppm, δ_C 77.0 ppm) as an internal standard. ESIMS and HRESIMS spectra were recorded on a Q-TOF Micro LC-MS-MS mass spectrometer. Reversed phase HPLC (Agilent 1100 series liquid chromatography using a VWD G1314A detector at 210 nm and a semipreparative ODS-HG-5 [5 μm, 10 mm (i.d.) × 25 cm] column) was also employed. Commercial Si gel (Qing Dao Hai Yang Chemical Group Co., 200-300 and 400-600 mesh) and Sephadex LH-20 (Amersham Biosciences) was used for column chromatography, and precoated Si gel plates (Yan Tai Zi Fu Chemical Group Co., G60 F-254) were used for analytical TLC. X-ray diffraction studies were carried out on a Bruker APEX2 CCD diffractometer.

3.2. Biological material

The specimens of *S. trocheliophorum*, identified by Prof. H. Huang of the South China Sea Institute of Oceanology, Chinese Academy of Sciences (CAS), were collected by scuba at Yalong Bay, Hainan Province, China, in February 26, 2006, at a depth of −20 m, and were frozen immediately after collection. A voucher specimen is available for inspection at the Shanghai Institute of Materia Medica, CAS, under registration No. YAL-62.

3.3. Extraction and isolation

The frozen animals (301 g, dry weight) were cut into pieces and extracted exhaustively with Me_2CO at room temperature (3 × 1.5 l, 15 min in ultrasonic bath). The organic extract was evaporated to give a brown residue, which was partitioned between Et_2O and H_2O. The Et_2O solution was concentrated under reduced pressure to give a dark brown residue (3.5 g), which was fractionated by gradient Si gel (200-300 mesh) column chromatography (CC) (0 → 100% Et_2O in petroleum ether (PE)), yielding twenty-one fractions (A – U). Each of fractions J and M was subjected to silica gel (400-600 mesh) CC (PE/Et_2O 25:1 and PE/Me_2CO 30:1, respectively) to give **11** (13.8 mg) and **12** (23.0 mg), respectively. Fraction N was purified by CC (*Sephadex LH-20*, PE/$CHCl_3$/MeOH 2:1:1), followed by CC (silica gel (400-600 mesh), PE/Me_2CO, 10:1)) to afford two sub-fractions N1 and N2. Sub-fraction N1 was successively separated by reversed-phase HPLC [semi-prep. ODS-HG-5 (5 μm, 250 × 9.4 mm), MeCN/H_2O (67:33), 2.0 ml/min] to afford **8** (12.0 mg; t_R 39.1 min). Similarly, **2** (10.2 mg; t_R 27.3 min) and **3** (6.6 mg; t_R 29.1 min) were obtained from sub-fraction N2 by reversed-phase HPLC [semi-prep. ODS-HG-5 (5 μm, 250 × 9.4 mm), MeCN/H_2O (70:33), 2.0 ml/min]. Fraction O was further divided into three sub-fractions O1, O2, and O3 (56.1 mg, 107.2 mg, and 72.7 mg, respectively) by CC (sillica gel (400-600 mesh), PE/Et_2O, 2:1 → 1:1)). Sub-fraction O2 was then purified by reversed-phase HPLC [semi-prep. ODS-HG-5 (5 μm, 250 × 9.4 mm), MeCN/H_2O (80:20), 2.0 ml/min] yielding **9** (26.3 mg; t_R 17.0 min), and **10** (54.7 mg; t_R 15.6 min) and a mixture of residue, from which **1** (1.9 mg; t_R 22.5 min) was obtained by the further purification using reversed-phase HPLC [semi-prep. ODS-HG-5 (5 μm, 250 × 9.4 mm), MeOH/H_2O (85:15), 2.0 ml/min]. Fraction P was subjected to a column of *Sephadex LH-20* eluting with PE/$CHCl_3$/MeOH (2:1:1) to give five sub-fractions P1–P5 (13.9 mg, 43.7 mg, 59.9 mg, 39.8 mg, 19.3 mg, respectively). Sub-fraction P4 was successively separated by reversed-phase HPLC [semi-prep. ODS-HG-5 (5 μm, 250 × 9.4 mm), MeCN/H_2O (70:30), 2.0 ml/min] yielding **4** (4.3 mg; t_R 9.8 min) and **13** (1.1 mg; t_R 20.4 min). Two sub-fractions Q1 and O2 (84.3 mg, 56.9 mg, respectively) were got from fraction Q by CC

(*Sephadex LH-20*, PE/$CHCl_3$/MeOH 2:1:1). Sub-fraction Q1 was further purified by reversed-phase HPLC [semi-prep. ODS-HG-5 (5 µm, 250 × 9.4 mm), MeCN/H_2O (53:47), 2.0 ml/min] to **6** (2.9 mg; t_R 14.6 min) and **7** (7.5 mg; t_R 34.2 min). Similarly, **5** (4.3 mg; t_R 23.3 min) was obtained from sub-fraction Q2 by reversed-phase HPLC [semi-prep. ODS-HG-5 (5 µm, 250 × 9.4 mm), MeCN/H_2O (45:55), 2.0 ml/min].

*3.3.1 Sarcophytonolide S (**1**):* colorless oil. $[\alpha]_D^{20}$ = +112.0 (*c* = 0.08, $CHCl_3$). UV (MeOH): 283 (3.33). ECD {MeCN, λ [nm] (Δε), c 0.153 mM}: 313sh (+0.06), 283 (+0.34), 267sh (+0.26), 223sh (+0.43), 209 (+0.96), 200 (+1.14). IR (KBr): 3498, 2958, 2930, 1713, 1636, 1070. ^{1}H- and ^{13}C-NMR, see Table 1. ESI-MS: 371.3 ([M + Na]$^+$). HR-ESI-MS: 371.2172 ([M + Na]$^+$, $C_{21}H_{32}NaO_4^+$; calc. 371.2198).

*3.3.2 Sarcophytonolide T (**2**):* colorless oil. $[\alpha]_D^{20}$ = +42.5 (*c* = 0.12, $CHCl_3$). IR (KBr): 2958, 1714, 1629, 1037, 940, 745. ^{1}H- and ^{13}C-NMR, see Table 1. ESI-MS: 399.3 ([M + Na]$^+$). HR-ESI-MS: 399.2146 ([M + Na]$^+$, $C_{22}H_{32}NaO_5^+$; calc. 399.2147).

*3.3.3 Sarcophytonolide U (**3**):* colorless oil. $[\alpha]_D^{22}$ = +355.5 (*c* = 0.11, $CHCl_3$). UV ($CHCl_3$): 238 (3.82), 286 (3.97). ECD {MeCN, λ [nm] (Δε), c 0.147 mM}: 292sh (+0.87), 282 (+1.00), 269sh (+0.69), 237 (+0.32), 222sh (-0.11), 213 (-0.33) , 203 (-0.55) , 195sh (-0.25). IR (KBr): 2957, 1716, 1634, 1076, 761. ^{1}H- and ^{13}C-NMR, see Table 1. ESI-MS: 399.3 ([M + Na]$^+$). HR-ESI-MS: 399.2176 ([M + Na]$^+$, $C_{22}H_{32}NaO_5^+$; calc. 399.2147).

*3.3.4 Sartrolide H (**4**):* Colorless oil. $[\alpha]_D^{20}$ = +78 .0 (*c* = 0.11, $CHCl_3$). ECD {MeCN, λ [nm] (Δε), c 0.122 mM}: 314sh (+0.12), 296 (+0.26), 270sh (-0.43), 262 (-0.60), 232 (+2.34), 204 (+6.34), 199sh (+5.44). IR (KBr): 3463, 2924, 1670, 1640, 1067, 947, 751. ^{1}H-NMR ($CDCl_3$, 400 MHz): *δ* 5.38 (1H, *d*, *J* = 9.6 Hz, H-2), 3.62 (1H, *d*, *J* = 9.6 Hz, H-3), 2.98 (1H, *dd*, *J* = 10.4, 4.3 Hz, H-5), 2.25 (1H, *m*, H_a-6), 1.60 (1H, *ddd*, *J* = 14.7, 10.5, 2.1 Hz, H_b-6), 4.08 (1H, *d*, *J* = 12.5 Hz, H-7), 2.18 (1H, *m*, H_a-9), 2.04 (1H, *m*, H_b-9), 2.49 (1H, *m*, H_2-10), 6.21 (1H, *t*, *J* = 4.5 Hz, H-11), 3.06 (1H, *d*, *J* = 14.1 Hz, H_a-13), 2.29 (1H, *m*, H_b-13), 2.61 (1H, *t*, *J* = 13.9 Hz, H_a-14), 2.21 (1H, *m*, H_b-14), 2.46 (1H, *m*, H-15), 1.07 (3H, *d*, *J* = 7.3 Hz, Me-16), 1.09 (3H, *d*, *J* = 7.3 Hz, Me-17), 1.41 (3H, *s*, Me-18), 1.38 (3H, *s*, Me-19), 3.26 (3H, *s*, Me-1´). ^{13}C-NMR ($CDCl_3$, 100 MHz): *δ* 152.5 (*s*, C-1), 119.6 (*d*, C-2), 75.4 (*d*, C-3), 63.1 (*s*, C-4), 60.2 (*d*, C-5), 30.4 (*t*, C-6), 69.1 (*d*, C-7), 82.9 (*s*, C-8), 34.6 (*t*, C-9), 26.7 (*t*, C-10), 141.2 (*d*, C-11), 132.4 (*s*, C-12), 33.8 (*t*, C-13), 28.1 (*t*, C-14), 30.3 (*d*, C-15), 23.2 (*q*, C-16), 20.9 (*q*, C-17), 17.8 (*q*, C-18), 22.7 (*q*, C-19), 166.3 (*s*, C-20), 56.2 (*q*, C-1´). ESI-MS: 387.2 ([M + Na]$^+$). HR-ESI-MS: 387.2158 ([M + Na]$^+$, $C_{21}H_{32}NaO_5^+$; calc. 387.2147).

*3.3.5 Sartrolide I (**5**):* Colorless oil. $[\alpha]_D^{20}$ = +18.7 (*c* = 0.11, $CHCl_3$). IR (KBr): 3478, 2927, 1710, 1667, 1635, 1065, 948 750. ^{1}H- and ^{13}C-NMR, see Table 2. EI-MS: 417.3 ([M + Na]$^+$). HR-ESI-MS: 417.2236 ([M + Na]$^+$, $C_{22}H_{34}NaO_6^+$; calc. 417.2253).

*3.3.6 Sartrolide J (**6**):* Colorless oil. $[\alpha]_D^{20}$ = +12.5 (*c* = 0.09, $CHCl_3$). IR (KBr): 3483, 2929, 1707, 1664, 1639, 1069, 944, 753. ^{1}H- and ^{13}C-NMR: *Table 2*. ESI-MS: 417.3 (100, [*M* + Na]$^+$). HR-ESI-MS *m/z* 417.2269 ([M + Na]$^+$, $C_{22}H_{34}NaO_6^+$; calc. 417.2253).

*3.3.7 Deacetylemblide (**7**):* Colorless oil. $[\alpha]_D^{22}$ +88.0 (*c* = 0.11, $CHCl_3$). IR (KBr): 3457, 1717, 1672, 1636, 1069, 952, 746. ^{13}C-NMR ($CDCl_3$, 100 MHz): *δ* 155.9 (*s*, C-1), 120.0 (*d*, C-2), 135.3 (*d*, C-3), 124.8 (*s*, C-4), 25.6 (*t*, C-5), 27.5 (*t*, C-6), 65.3 (*d*, C-7), 83.3 (*s*, C-8), 34.4 (*t*, C-9), 27.0 (*t*, C-10), 142.3 (*d*, C-11), 132.1 (*s*, C-12), 36.7 (*t*, C-13), 27.7 (*t*, C-14), 35.3 (*d*, C-15), 21.8 (*q*, C-16), 22.1 (*q*, C-17), 170.0 (*s*, C-18), 22.9 (*q*, C-19), 166.6 (*s*, C-20), 51.6 (*q*, C-1´). ESI-MS: 385.3 ([M + Na]$^+$).

*3.3.8 4Z,12Z,14E-Sarcophytolide (**8**):* Colorless crystals (MeOH). m.p. 121.3 – 122.8°. $[\alpha]_D^{22}$ = +132.1 (*c* = 0.11, CH_2Cl_2). ECD {MeCN, λ [nm] (Δε), c 0.268 mM}: 277sh (+4.58), 262sh (+15.08), 257sh (+22.53), 248sh (+39.00), 241 (+45.68), 225sh (-19.09), 217 (-32.69), 209sh (-24.75), 192 (-18.03). ECD {(37 µg in 250 mg KCl), λ [nm] (Φ)}: 319 (-1.32), 285sh (+3.52), 273sh (+9.32), 259sh (+33.49), 250sh (+58.00), 243 (+67.10), 222sh (-42.65), 217 (-48.59), 208sh (-35.69), 192 (-26.34).

*3.3.9 Sarcrassin D (**9**):* Colorless crystals (MeOH). m.p. 113.5 – 115.1°. $[\alpha]_D^{22}$ = +180.1 (*c* 0.10, $CHCl_3$). ECD {MeCN, λ [nm] (Δε), c 0.149 mM}: 296sh (+4.56), 286sh (+7.50), 276 (+8.55), 263sh (+7.77), 253sh (+6.58), 241sh (+5.47), 216 (-5.17). ECD {49 µg in 250 mg KCl, λ [nm] (Φ)}: 314sh (+0.61), 304sh (+3.86), 291sh (+9.18), 281 (+10.74), 273sh (+9.79), 245sh (+5.92), 242sh (+5.78), 217sh (-10.62), 211 (-11.37).

*3.3.10 Emblide (**10**):* Colorless crystals (MeOH). m.p. 121.5 – 123.1°. $[\alpha]_D^{20}$ = +154.5 (*c* = 0.11, $CHCl_3$). ECD {MeCN, λ [nm] (Δε), c 0.270 mM}: 305sh (+4.75), 295sh (+9.67), 279 (+14.23), 266sh (+10.78), 258sh (+5.67), 238sh (-4.34), 220 (-15.38), 208sh (-10.71), 193sh (+5.77). ECD {58 µg in 250 mg KCl, λ [nm] (Φ)}: 320sh (+1.06), 297sh (+13.36), 279 (+25.67), 263sh (+13.86), 248sh (-3.17), 221 (-29.29), 215sh (-27.76), 205sh (-13.33), 195sh (+9.42).

3.4. X-ray crystallographic analysis

Colorless blocks, $C_{20}H_{28}O_3$, M_r = 316.42, monoclinic, crystal size 0.14 × 0.10 × 0.08 mm, space group *P*2(1), *a* = 9.7253 (2) Å, *b* = 9.2859 (2) Å, *c* = 10.5777 (2) Å, *V* = 870.44 (3) Å^3, *Z* = 2, D_{calcd} = 1.207 mg m^{-3}, F_{000} = 344, 5713 collected reflections, 2589 unique reflections (R_{int} = 0.034), final R1 = 0.0329 (wR2 = 0.0900) for 2567 reflections with $I > 2\sigma(I)$, R1 = 0.0332, wR2 = 0.0906 for all unique data. The X-ray measurements were made on a Bruker APEX2 CCD X-ray diffractometer with graphite-monochromated Cu Kα (*λ* =1.54178 Å) radiation at 133(2) K. The structure was solved by direct methods (SHELXS-97) and refined with full-matrix least-squares on F^2 (SHELXL-97). The non-hydrogen atoms were refined anisotropically. All H atoms were located in a difference Fourier map, but they were introduced in calculated positions and treated as riding on their parent atoms [C–H = 0.93-0.97 Å, O–H = 0.82 Å, and U_{iso}(H) = 1.2U_{eq}(C) and 1.51U_{eq}-(C, O)]. CCDC 920814 contains the supplementary crystallographic data for this compound. These data can be obtained free of charge from *Cambridge Crystallographic Data Centre via* www.ccdc.can.ac.uk/data request/cif.

3.5. Computational section

Geometry optimizations [B3LYP/6-31G(d) *in vacuo*, B3LYP/TZVP, B97D/TZVP[16,18] and CAM-B3LYP/TZVP[19,20] with PCM solvent model for MeCN or $CHCl_3$] and TDDFT calculations were performed with Gaussian 09[34] using various functionals (B3LYP, BH&HLYP, CAM-B3LYP and PBE0) and TZVP basis set. ECD spectra were generated as the sum of Gaussians[35] with 4200 to 2400 cm^{-1} half-height width (corresponding to *c.a.* 20-12 nm at 220 nm), using dipole-velocity computed rotational strengths. Mixed torsional/low mode conformational searches were carried out by means of the Macromodel 9.9.223[36] software using Merck Molecular Force Field (MMFF) with implicit solvent model for $CHCl_3$ applying a 21 kJ/mol energy window. Boltzmann distributions were estimated from the B3LYP, B97D and CAM-B3LYP energies. In the case of the B3LYP/6-31G(d) *in vacuo* level ZPVE corrections were applied. The MOLEKEL[37] software package was used for visualization of the results.

3.6. PTP1B inhibitory activity assay

Recombinant PTP1B catalytic domain was expressed and purified according to a previous report.[38] The enzymatic activities of the PTP1B catalytic domain were determined at 30 °C by monitoring the hydrolysis of *p*NPP. Dephosphorylation of *p*NPP generates product *p*NP, which was monitored at an absorbance of 405 nm by the EnVision multilabel plate reader (PerkinElmer Life Sciences, Boston, MA). In a typical 100 μL assay mixture containing 50 mmol/L 3-[*N*-morpholino] propanesulfonic acid (MOPs), pH 6.5, 2 mmol/L *p*NPP, and 30 nmol/L recombinant PTP1B, activities were continuously monitored and the initial rate of the hydrolysis was determined using the early linear region of the enzymatic reaction kinetic curve. The IC_{50} was calculated with Prism 4 software (Graphpad, San Diego, CA) from the nonlinear curve fitting of the percentage of inhibition (% inhibition) versus the inhibitor concentration [I] by using the following equation: % Inhibition = $100/(1 + [IC_{50}/[I]]^k)$, where k is the Hill coefficient. The positive control is oleanolic acid (IC_{50} value is 2.56 ± 0.20 μM).

3.7. Antibacterial activity assay

The antimicrobial activities of natural products against *Staphylococcus aureus* Newman strain were performed by paper disk diffusion antimicrobial susceptibility test[39] and MIC (Minimum Inhibitory Concentration) method, respectively. Zones of inhibition were measured after 24 hr of incubation at 37ºC. For the MIC method, all the natural products were dissolved in DMSO (Dimethyl Sulphoxide) and diluted with culture broth to a concentration of 0.5 mg/mL. Further 1:2 serial dilutions were performed by addition of culture broth to reach concentrations ranging from 0.5 to 0.0156 mg/mL; 100 μL of each dilution were distributed in 96-well plates, as well as a sterility control and a growth control (containing culture broth plus DMSO, without natural products). Each test and growth control well was inoculated with 5 μL of a bacterial suspension (10^5 CFU/well). The 96-well plates were incubated at 37ºC for 24 h. MIC of the natural products against *Staphylococcus aureus* Newman strain was defined as the lowest concentration of each natural product, which completely inhibited bacterial growth. The positive control is fosfomycin sodium (MIC_{50} = 137.4 μM).

Acknowledgements

This research work was financially supported by the Natural Science Foundation of China (Nos. 41506187, 81520108028, 21672230), NSFC-Shandong Joint Fund for Marine Science Research Centers (No. U1606403), SCTSM Project (No. 15431901000), the Project Supported by Scientific Research Fund of Hunan Provincial Education Department (No. 16C1674), the SKLDR/SIMM Projects (SIMM 1705ZZ-01). The research of the Hungarian authors was supported by the EU and co-financed by the European Regional Development Fund under the project GINOP-2.3.2-15-2016-00008. The Governmental Information-Technology Development Agency (KIFÜ) is acknowledged for CPU time. We thank Prof. Ernesto Mollo from Institute of Biomolecular Chemistry (ICB) of the National Research Council (CNR), Italy, for the biological sample collection.

Appendix A. Supplementary data

Supplementary data related to this article can be found at http://dx.doi.org/10.1016/j.tet.XXXX.XX.XXXX.

References and notes

1. Liang, L.-F.; Guo, Y.-W. *Chem. Biodivers.* 2013, *10*, 2161-2196.
2. Anjaneyulu, A. S. R.; Rao, G. V. *J. Indian Chem. Soc.* 1997, *74*, 272-278.
3. Li, Y.; Pattenden, G. *Tetrahedron* 2011, *67*, 10045-10052.
4. Takamura, H.; Iwamoto, K.; Nakao, E.; Kadota, I. *Org. Lett.* 2013, *15*, 1108-1111.
5. Liang, L.-F.; Kurtán, T.; Mándi, A.; Yao, L.-G.; Li, J.; Zhang, W.; Guo, Y.-W. *Org. Lett.* 2013, *15*, 274-277.
6. Jia, R.; Kurtán, T.; Mándi, A.; Yan, X.-H.; Zhang, W.; Guo, Y.-W. *J. Org. Chem.* 2013, *78*, 3113-3119.
7. Huang, R.-Y.; Chen, W.-T.; Kurtán, T.; Mándi, A.; Ding, J.; Li, J.; Li, X.-W.; Guo, Y.-W. *Future Med. Chem.* 2016, *8*, 17-27.
8. Li, X.-W.; Chen, S.-H.; Ye, F.; Mollo, E.; Zhu, W.-L.; Liu, H.-L.; Guo, Y.-W. *Tetrahedron* 2017, *73*, 5239-5243.
9. Ye, F.; Zhu, Z.-D.; Chen, J.-S.; Li, J.; Gu, Y.-C.; Zhu, W.-L.; Li, X.-W.; Guo, Y.-W. *Org. Lett.* 2017, *19*, 4183-4186.
10. Liang, L.-F.; Kurtán, T.; Mándi, A.; Gao, L.-X.; Li, J.; Zhang, W.; Guo, Y.-W. *Eur. J. Org. Chem.* 2014, *2014*, 1841-1847.
11. Toth, J. A.; Burreson, B. J.; Scheuer, P. J.; Finer-Moore, J.; Clardy, J. *Tetrahedron* 1980, *36*, 1307-1309.
12. Gross, H.; Wright, A. D.; Beil, W.; König, G. M. *Org. Biomol. Chem.* 2004, *2*, 1133-1138.
13. Zhang, C.-X.; Li, J.; Su, J.-Y.; Liang, Y.-J.; Yang, X.-P.; Zheng, K.-C.; Zeng, L.-M. *J. Nat. Prod.* 2006, *69*, 1476-1480.
14. Jia, R.; Guo, Y.-W.; Mollo, E.; Cimino, G. *Helv. Chim. Acta* 2005, *88*, 1028-1033.
15. Bowden, B. F.; Coll, J. C.; Mitchell, S. J. *Aust. J. Chem.* 1980, *33*, 879-884.
16. Sun, P.; Xu, D.-X.; Mándi, A.; Kurtán, T.; Li, T.-J.; Schulz, B.; Zhang, W. *J. Org. Chem.* 2013, *78*, 7030-7047.
17. Li, C.; La, M.-P.; Sun, P.; Kurtan, T.; Mandi, A.; Tang, H.; Liu, B.-S.; Yi, Y.-H.; Li, L.; Zhang, W. *Mar. Drugs* 2011, *9*, 1403-1418.
18. Grimme, S. *J. Comput. Chem.* 2006, *27*, 1787-1799.
19. Yanai, T.; Tew, D. P.; Handy, N. C. *Chem. Phys. Lett.* 2004, *393*, 51-57.
20. Pescitelli, G.; Di Bari, L.; Berova, N. *Chem. Soc. Rev.* 2011, *40*, 4603-4625.
21. Polavarapu, P. L. *Chirality* 2008, *20*, 664-672.
22. Mándi, A.; Swamy, M. M. M.; Taniguchi, T.; Anetai, M.; Monde, K. *Chirality* 2016, *28*, 453-459.
23. Sun, P.; Yu, Q.; Li, J.; Riccio, R.; Lauro, G.; Bifulco, G.; Kurtán, T.; Mándi, A.; Tang, H.; Li, T.-J.; Zhuang, C.-L.; Gerwick, W. H.; Zhang, W. *J. Nat. Prod.* 2016, *79*, 2552-2558.
24. Liang, L.-F.; Gao, L.-X.; Li, J.; Taglialatela-Scafati, O.; Guo, Y.-W. *Bioorg. Med. Chem.* 2013, *21*, 5076-5080.
25. Liang, L.-F.; Lan, L.-F.; Taglialatela-Scafati, O.; Guo, Y.-W. *Tetrahedron* 2013, *69*, 7381-7386.
26. Mao, S.-C.; Guo, Y.-W.; Shen, X. *Bioorg. Med. Chem. Lett.* 2006, *16*, 2947-2950.
27. Pescitelli, G.; Bruhn, T. *Chirality* 2016, *28*, 466-474.
28. Tursch, B.; Braekman, J. C.; Daloze, D.; Kaisin, M. In *Marine Natural Products: Chemical and Biological Perspectives;* Scheuer, P. J. Ed.; Academic Press: New York, 1978; pp. 247-296.
29. Jia, R.; Guo, Y.-W.; Mollo, E.; Gavagnin, M.; Cimino, G. *J. Nat. Prod.* 2006, *69*, 819-822.
30. Zhang, W.; Krohn, K.; Ding, J.; Miao, Z.-H.; Zhou, X.-H.; Chen, S.-H.; Pescitelli, G.; Salvadori, P.; Kurtan, T.; Guo, Y.-W. *J. Nat. Prod.* 2008, *71*, 961-966.
31. Wang, J.-R.; Carbone, M.; Gavagnin, M.; Mándi, A.; Antus, S.; Yao, L.-G.; Cimino, G.; Kurtán, T.; Guo, Y.-W. *Eur. J. Org. Chem.* 2012, *2012*, 1107-1111.
32. Kurtán, T.; Jia, R.; Li, Y.; Pescitelli, G.; Guo, Y.-W. *Eur. J. Org. Chem.* 2012, *2012*, 6722-6728.
33. Jiang, C.-S.; Liang, L.-F.; Guo, Y.-W. *Acta Pharmacol. Sin.* 2012, *33*, 1217-1245.
34. M. J. Frisch, G. W. Trucks, H. B. Schlegel, G. E. Scuseria, M. A. Robb, J. R. Cheeseman, G. Scalmani, V. Barone, B. Mennucci, G. A. Petersson, H. Nakatsuji, M. Caricato, X. Li, H. P. Hratchian, A. F. Izmaylov, J. Bloino, G. Zheng, J. L. Sonnenberg, M. Hada, M. Ehara, K. Toyota, R. Fukuda, J. Hasegawa, M. Ishida, T. Nakajima, Y. Honda, O. Kitao, H. Nakai, T. Vreven, J. A. Montgomery Jr., J. E. Peralta, F. Ogliaro, M. Bearpark, J. J. Heyd, E. Brothers, K. N. Kudin, V. N. Staroverov, R. Kobayashi, J. Normand, K. Raghavachari, A. Rendell, J. C. Burant, S. S. Iyengar, J. Tomasi, M. Cossi, N. Rega, J. M. Millam, M. Klene, J. E. Knox, J. B. Cross, V. Bakken, C. Adamo, J. Jaramillo, R. Gomperts, R. E. Stratmann, O. Yazyev, A. J. Austin, R. Cammi, C. Pomelli, J. W. Ochterski, R. L. Martin, K. Morokuma, V. G. Zakrzewski, G. A. Voth, P. Salvador, J. J. Dannenberg, S. Dapprich, A. D. Daniels, Ö.

Farkas, J. B. Foresman, J. V. Ortiz, J. Cioslowski, D. J. Fox, Gaussian 09, revision B.01, Gaussian, Inc., Wallingford CT, 2010.
35. Stephens, P. J.; Harada, N. *Chirality* 2010, *22*, 229-233.
36. MacroModel; Schrödinger LLC, 2012; https://www.schrodinger.com/MacroModel.
37. U. Varetto, MOLEKEL 5.4; Swiss National Supercomputing Centre: Manno, Switzerland, 2009.
38. Yang, X.-N.; Li, J.-Y.; Zhou, Y.-Y.; Shen, Q.; Chen, J.-W.; Li, J. *Biochim. Biophys. Acta - Gen. Subj.* 2005, *1726*, 34-41.
39. Bauer, A. W.; Kirby, W. M.; Sherris, J. C.; Turck, M. *Am. J. Clin. Pathol.* 1966, *45*, 493-496.